NOTE

Reducing the staircasing error in computational dosimetry of low-frequency electromagnetic fields

Ilkka Laakso and Akimasa Hirata

Nagoya Institute of Technology, Department of Computer Science and Engineering, Japan

E-mail: laakso.ilkka@nitech.ac.jp

Abstract. From extremely low frequencies to intermediate frequencies, the magnitude of induced electric field inside the human body is used as the metric for human protection. The induced electric field inside the body can be computed using anatomically realistic voxel models and numerical methods such as the finite-difference or finite-element methods. The computed electric field is affected by numerical errors that occur when curved boundaries with large contrasts in electrical conductivity are approximated using a staircase grid. In order to lessen the effect of the staircasing error, the use of the 99th percentile electric field, i.e., ignoring the highest 1 % of electric field values, is recommended in the ICNIRP guidelines. However, the 99th percentile approach is not applicable to localized exposure scenarios where the majority of significant induced electric field values may be concentrated in a small volume. In this paper, a method for removing the staircasing error is proposed. Unlike the 99th percentile, the proposed method is also applicable to localized exposure scenarios. The performance of the method is first verified by comparison with the analytical solution in a layered sphere. The method is then applied for six different exposure scenarios in two anatomically realistic human head models. The results show that the proposed method can provide conservative estimates for the 99th percentile electric field in both localized and uniform exposure scenarios.

Submitted to: *Phys. Med. Biol.*

1. Introduction

In electromagnetic dosimetry at low frequencies, the induced electric field inside the human body is used as the metric for the basic restriction limits in the ICNIRP (2010) guidelines and IEEE (2002) standard. The induced electric field can be simulated using numerical methods and anatomically realistic voxel models. However, numerical errors make the simulated maximum electric field values unreliable. The maximum electric field value depends on the resolution of the numerical grid and is susceptible to staircasing error that occurs when curved boundaries with large conductivity contrasts are approximated using rectilinear computational grids (Dawson *et al* 1997, Dawson *et al* 2001, Caputa *et al* 2002, Dimbylow 2005, Hirata *et al* 2010, Hirata *et al* 2011).

Dawson *et al* (2001) investigated several methods for lessening the impact of staircase approximation error by comparing numerical and analytic electric fields in several simple geometrical models. Of the proposed methods, the 99th percentile,

i.e., ignoring the highest 1 % of electric field values, has been adopted widely in later research and its use is recommended in the new ICNIRP (2010) guidelines. Using the 99th percentile value is effective in removing spurious electric field hotspots, which has been confirmed by comparing analytical and numerical electric fields in homogeneous and layered spheres exposed to a uniform magnetic field, and verifying that the analytical maximum and numerical 99th percentile electric field values are in a close agreement (Dawson *et al* 2001). Unlike the voxel maximum electric field values, the 99th percentile values are independent of the grid resolution in both simple geometries (Dawson *et al* 2001, Hirata *et al* 2011) and realistic body models (Caputa *et al* 2002, Hirata *et al* 2011).

There are several problems with the 99th percentile approach. In addition to excluding potentially erroneous values, 99th percentile may also exclude values that are real and should not be ignored. Hence, the 99th percentile electric field only makes sense for uniform exposure when all parts of the tissues are exposed relatively uniformly. For instance, during localized magnetic-field exposure, ignoring the highest 1 % could lead to significant underestimation of the real exposure as majority of significant electric field values might be included in the highest 1 % (an analytical example is shown in section 3.1). In order to remove the underestimation caused by the 99th percentile, Kos *et al* (2011) have used the 999th permille for the whole body instead of the 99th percentile when studying the exposure to the magnetic field of an induction cooker. Percentile value also depends on the volume over which the percentile is taken. For example, if the left side of the body were more exposed than the right side, then the 99th percentile value would inevitably be smaller if taken over the whole brain (as recommended by ICNIRP (2010)) instead of only the left side.

In this paper, a simple algorithm for reducing the staircasing error is proposed. The algorithm is based "smoothing" the body conductivity values reducing the conductivity contrast between adjacent tissues. When the smoothing algorithm is applied, the 99th percentile electric field values will stay unchanged but the maximum values will become more realistic, which is verified by comparison with the analytic solution in a layered sphere in section 3.1. The smoothing algorithm is applied for realistic exposure cases in section 3.2, where two different anatomically realistic head models are exposed to six different localized and uniform magnetic field distributions.

2. Methods

2.1. Scalar-potential equation

Assume that a conducting object, such as the human body, is exposed to an external a low-frequency magnetic field with magnetic flux density $\mathbf{B}_0$. When the external magnetic field is changing slowly and the conductivity is relatively low, it can be assumed that the induced currents do not perturb the external magnetic field. Then the electric field $\mathbf{E} = -\nabla\phi - \mathbf{A}_0$, where the vector potential $\mathbf{A}_0$ satisfies $\nabla \times \mathbf{A}_0 = \frac{\partial}{\partial t}\mathbf{B}_0$, and the electric scalar potential ϕ can be solved (Dawson *et al* 1996, Dawson and Stuchly 1998) from

$$\nabla \cdot \sigma\nabla\phi = -\nabla \cdot \sigma\mathbf{A}_0, \tag{1}$$

where σ is the conductivity. The incoming vector potential $\mathbf{A}_0$ for (1) can be calculated using the Biot-Savart law, or by selecting a suitable $\mathbf{A}_0$ when the incident magnetic flux density $\mathbf{B}_0$ is simple.

2.2. Finite element method

In this study, equation (1) is solved numerically using the finite element method (FEM) with trilinear node-based basis functions in cubical elements, similarly to Ilvonen and Laakso (2009). The matrix equation is solved iteratively by the successive over-relaxation (SOR) iteration. Compared to the scalar-potential finite-difference (SPFD) method (Dawson *et al* 1996), the finite-element formulation used in this study requires more operations (21 nonzeros on each row of the system matrix compared to 7 in the SPFD method) but the SOR iteration converges slightly faster. The numerical accuracy (verified using the layered sphere of section 3.1) and memory requirements of the two methods are similar. Earlier, it has been reported that the SPFD produces results that are in good agreement with the quasi-static FDTD method and the impedance method (Dawson *et al* 1996, Dimbylow 1998).

2.3. Averaging of the electric field

The ICNIRP (2010) guidelines require taking a vector average of the electric field over $2 \times 2 \times 2$ mm^3 cubes. In this study, with piecewise trilinear basis functions and $2 \times 2 \times 2$ mm^3 voxels, the ICNIRP-averaged electric field in each voxel is the same as the electric field value at the centre point of the voxel. For the analytical solutions in section 3.1, the ICNIRP (2010) average of the analytical electric field was approximated as the pointwise electric field value at the centre of each voxel.

2.4. Algorithm for reducing staircasing error

Large contrasts in tissue conductivity between neighbouring voxels have been suggested to be the main reason for the staircase approximation error (Dawson *et al* 2001, Dimbylow 2005, Hirata *et al* 2010). The proposed algorithm for reducing the staircase approximation error consists in simply making the conductivity smoother, thus making the problem easier to solve numerically. The induced electric field values inside anatomical voxel models have been observed to remain relatively stable as compared with the current density when the conductivity values are modified (Dimbylow 2005, Bahr *et al* 2007).

In the proposed algorithm, the new smoothed conductivity σ_{smooth} in each voxel is a linear average of the original conductivity σ_{old} over a spherical volume

$$\sigma_{\mathrm{smooth}}(i,j,k) = \frac{1}{N} \sum_{B_n(i,j,k)} \sigma_{\mathrm{old}}, \tag{2}$$

where $B_n(i,j,k)$ is a voxelized sphere centred at the voxel (i,j,k) with a radius (the 'smoothing radius') of n voxels, consisting of a total of N voxels (N = 27, 93, 251, 485, and 895 for smoothing radii n = 2, 3, 4, 5, and 6, respectively). When the smoothing algorithm is applied, the air voxels in the vicinity of the body will get a small conductivity, which will result in violation of the condition that the induced electric field should be tangential on the (original) outer boundaries. Smoothing will also result in loss of anatomical details, but the smoothed conductivity values may still fall within the uncertainty range of low-frequency conductivity values (Gabriel *et al* 2009).

Implementation of the smoothing algorithm is straightforward. The new conductivity is simply used in place of the original conductivity in existing SPFD and FEM solvers. Because the smoothing algorithm is essentially a convolution

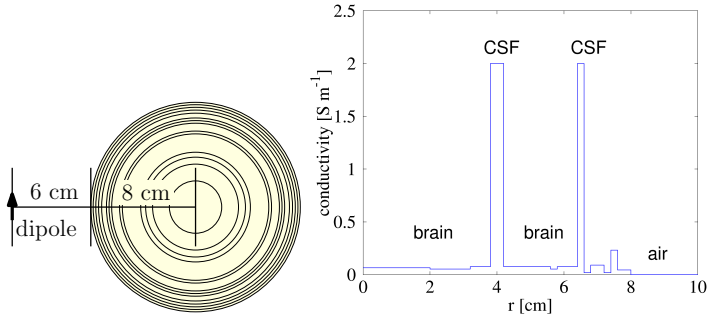

Figure 1. Location and direction of the magnetic dipole (left) and the conductivity as a function of radius for the layered sphere (right).

between the characteristic function of a n-radius voxelized sphere and the original 3-dimensional conductivity, it can be performed using quick numerical methods for calculating convolution.

3. Results

3.1. Comparison with analytic solutions in a layered sphere

The first numerical example is a layered sphere exposed to the quasistatic magnetic field of an infinitesimally short magnetic dipole that is located 6 cm away from the sphere (figure 1). The analytic solution for this kind of geometry can be obtained from the Maxwell equations even for an arbitrary external magnetic field. The sphere consists of 13 layers with conductivity as shown in figure 1. The thickness of each layer is a multiple of 2 mm. The conductivity profile of the sphere was originally taken from the side of the head of the TARO voxel model. The sphere was divided into $2 \times 2 \times 2$ mm^3 cubical voxels.

Figure 2 shows the amplitude of the induced electric field on a cross-section of the sphere for various smoothing radii. The source dipole is located above the figures with the dipole moment perpendicular to the cross-section plane. The colour scale ranges from blue (low) to red (high), and it has been scaled similarly in each figure. The significance of the staircasing error becomes clear when comparing the analytical solution (a) to the case with no smoothing (b). When applying the smoothing algorithm (c,d), the error compared to the analytic solution is greatly reduced, almost disappearing when the smoothing radius is six cells (d).

Figure 3 shows comparison between the analytic and numerical electric field in the brain tissues (left) and over the whole sphere (right). The value of 100 % in each figure corresponds to the analytical maximum electric field value. In this kind of a localized exposure scenario, the 99th percentile is unable to give a good approximation of the maximum value: The analytical 99th percentile value in the brain tissues is 30 % lower than the maximum value, and when taken over the whole sphere, the 99th percentile underestimates the maximum value by 40 %. If the dipole were located closer to the sphere, the difference would become even more pronounced. On the contrary, for uniform magnetic field exposure of a layered sphere, the analytical maximum and 99th percentile values would agree very well (Dawson *et al* 2001, Hirata *et al* 2011).

As expected, analytical and numerical 99th percentile values are in a very good

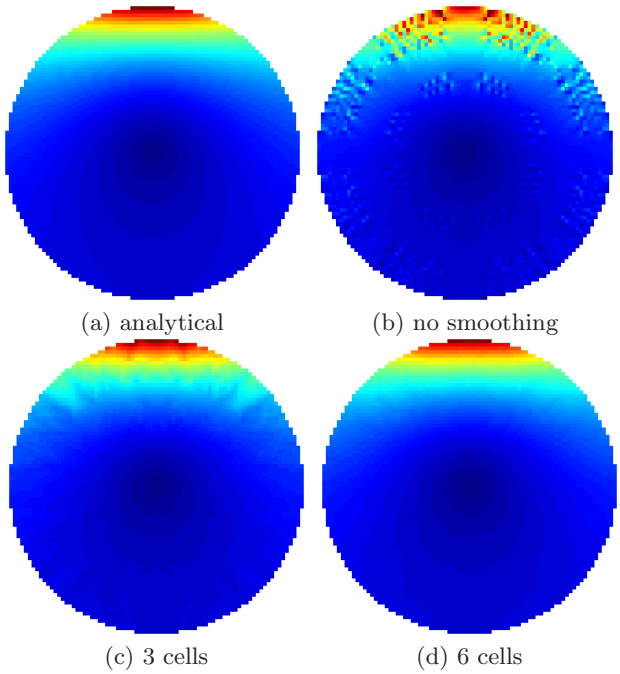

(a) analytical (b) no smoothing

(c) 3 cells (d) 6 cells

Figure 2. Amplitude of the induced electric field inside the layered sphere on the plane normal to the dipole moment.

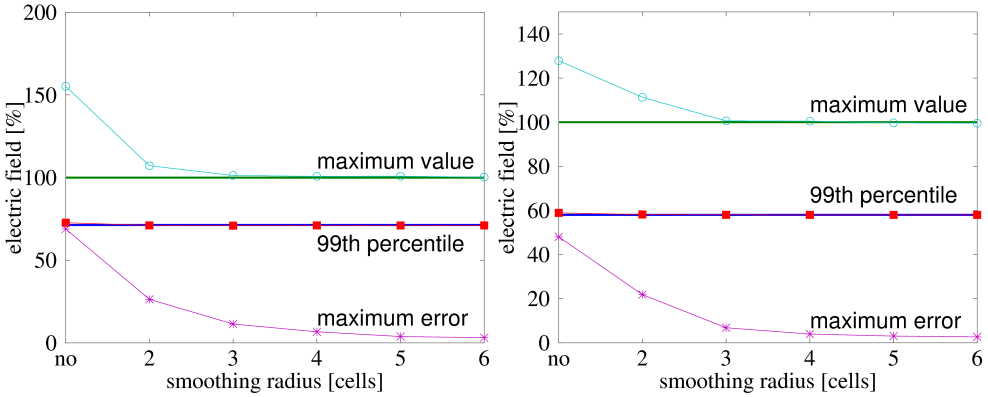

Figure 3. Comparison of the computed and analytical electric field in the brain tissue (left) and over all tissues (right) in the layered sphere. Thin lines with markers are the computed results, and the value of 100 % corresponds to the analytical maximum electric field.

agreement, even without smoothing (figure 3). On the contrary, the numerical maximum electric field values greatly overestimate the analytical maximum values because of the staircasing error. Applying smoothing quickly removes the error in the maximum values. The smoothing algorithm not only removes the error in the maximum values but also in the global error measured in terms of the maximum

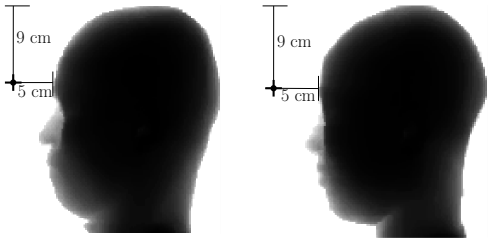

Figure 4. Location of the dipole for TARO (left) and HANAKO (right) models.

norm, i.e.,

$$\text{maximum error} = \max |\mathbf{E}_{\text{numerical}} - \mathbf{E}_{\text{analytical}}|, \tag{3}$$

where the maximum value is taken over the whole brain tissue (figure 3, left) or over the whole sphere (figure 3, right).

It is clear from figures 2 and 3 that applying even a slight smoothing with a smoothing radius of 3 cells can remove the worst staircase approximation errors for a smooth geometry such as the sphere. In addition to reduced staircasing error, the SOR iteration seemed to converge up to 2 times faster when the conductivity was smoother. The same tendency was also present when using anatomically realistic models (section 3.2). The reduction in computational time is especially advantageous for large problems featuring anatomically realistic whole-body models.

3.2. Uniform and localized exposure of anatomically realistic head models

In this section, the smoothing algorithm is applied for anatomically realistic head models exposed to both uniform and localized power-frequency magnetic fields. Japanese adult male (TARO) and female (HANAKO) models (Nagaoka *et al* 2004) with conductivity values taken from (Gabriel *et al* 1996) at a frequency of 50 Hz are used as the human body models. Only the heads of the models are considered. The TARO and HANAKO models have been used previously in low-frequency dosimetry in several studies (Ilvonen and Laakso 2009, Hirata *et al* 2009, Hirata *et al* 2010, Dimbylow and Findlay 2010).

A total of six different exposure conditions, three uniform and three localized, are investigated. In the uniform exposure cases, the head is exposed to a homogeneous magnetic flux density of 10 mT (the ICNIRP reference level for occupational exposure) in three orthogonal directions: antero-posterior (AP), top-to-bottom (TOP) and lateral (LAT). In the localized exposure scenarios, an infinitesimally short magnetic dipole is located 5 cm in front of the forehead of the model as shown in figure 4. The vertical position is 9 cm from the top of the head. The dipole moment has been scaled such that the highest magnetic flux density inside the body is 100 mT, which produces induced electric field comparable to the 10 mT uniform exposure. The direction of the dipole moment is varied in three orthogonal directions (AP, TOP and LAT). Collections of such magnetic dipoles can be used to represent inhomogeneous magnetic field distribution of real devices (Yamazaki *et al* 2004, Nishizawa *et al* 2007).

The induced electric field in the central nervous system (CNS) for the uniform and dipole exposures are shown in figures 5 and 6, respectively. The CNS consists of the brain, spinal chord, optic nerves and retinae. An example of the induced electric field

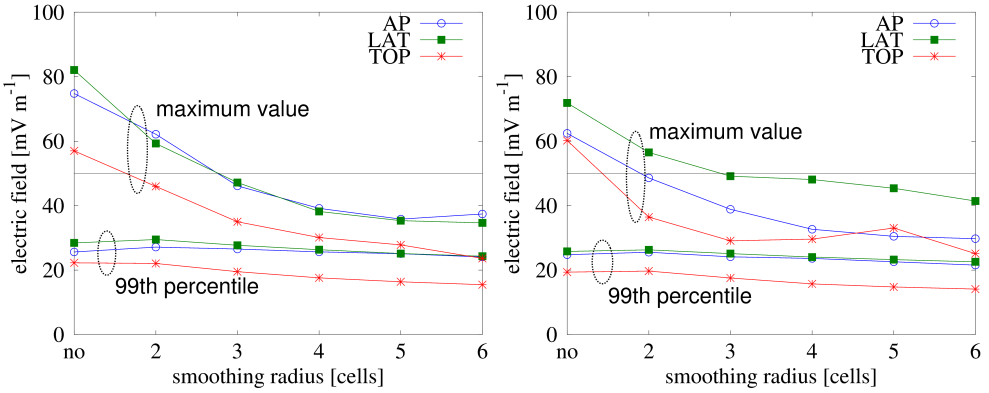

Figure 5. Uniform magnetic field exposure of 10 mT at 50 Hz. The induced electric field in the TARO (left) and HANAKO (right) models.

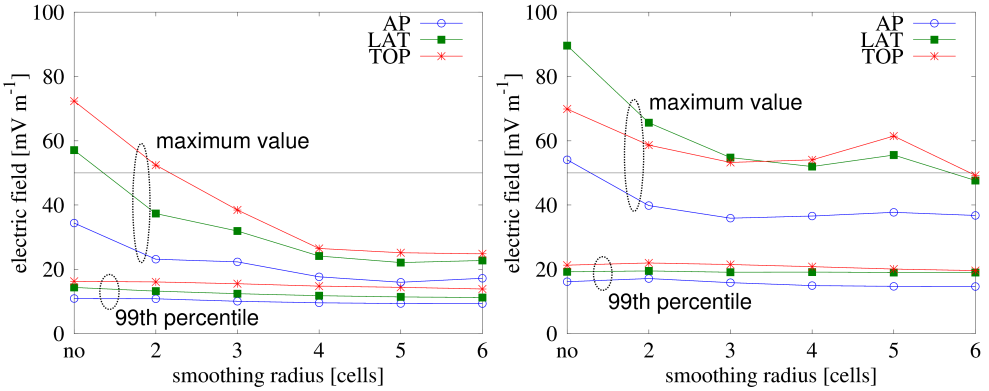

Figure 6. Exposure to short magnetic dipole located 5 cm away from the forehead. The induced electric field in the TARO (left) and HANAKO (right) models.

distribution for various smoothing radii is shown in figure 7 for the dipole exposure in the TOP direction.

Even though the heterogeneous geometry of the head is quite different from that of the layered sphere, the trend in the maximum induced electric field with the smoothing radius is similar (figures 5 and 6). The maximum electric field quickly decreases when the smoothing algorithm is applied until the smoothing radius is about 3–4 cells, after which the maximum value "converges". Typically the converged maximum value is 150–200 % of the 99th percentile value for the uniform exposure (figure 5), and 200–300 % for the dipole exposure (figure 6). Without smoothing, the maximum values would be about 250–300 % and 300–450 % of the 99th percentile for the uniform and dipole exposures, respectively. As illustrated in figure 7(a), high maximum values without smoothing can be attributed to just a few voxels with spurious electric field hotspots. These hotspots disappear when the smoothing algorithm is applied (b,c).

For the uniform exposure at the ICNIRP (2010) reference level of 10 mT, the 99th percentile electric field is in compliance with the basic restriction limit of 50 mV m^{-1} as excepted (figure 5). The maximum induced electric field values in the CNS would

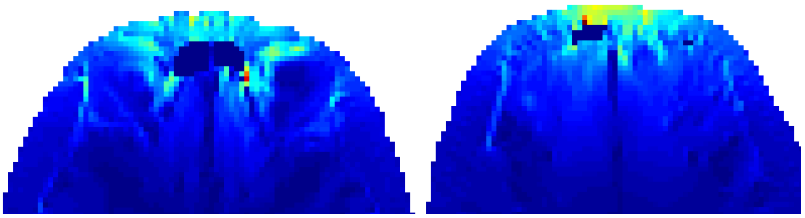

(a) no smoothing

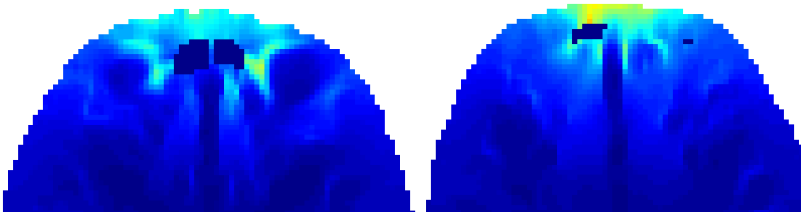

(b) 2 cells

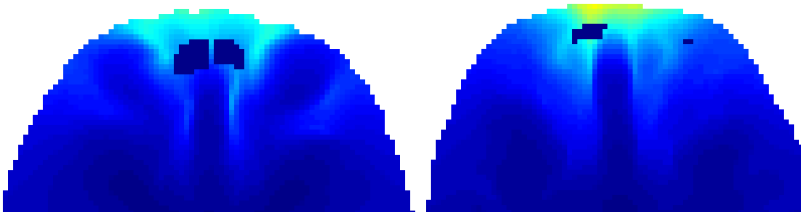

(c) 4 cells

Figure 7. Exposure to dipole in the TOP direction for the TARO (left column) and HANAKO (right column) models. The figures show the amplitude of the induced electric field on the horizontal cross section that has the highest maximum electric field in the CNS.

exceed the limit without smoothing. However, when the smoothing algorithm is applied, also the maximum electric fields decrease to values compliant with the basic restriction limit.

Similarly to the analytical case, the changes in the 99th percentile value with smoothing are small compared to the changes in the maximum induced electric field. The smoothed maximum electric field value is larger than the nonsmoothed 99th percentile value. Hence, the smoothed maximum electric field value acts as a conservative estimate for the 99th percentile value. The smoothed maximum value is also applicable to very localized exposure problems where using the 99th percentile makes little sense.

Unlike in the analytical case, the accuracy of the smoothed electric field remains unclear for the realistic case because no analytic solution exists. Nonetheless, large changes in the maximum values with smoothing underline the magnitude of numerical errors. In the ideal case, the numerical results should stay stable with respect to small changes in input parameters such as the conductivity, which is clearly not true in the current case.

4. Conclusions

A simple algorithm for reducing the numerical errors associated with staircase approximation in low-frequency electromagnetic dosimetry was presented. The algorithm is based on smoothing the electric conductivity of the body, which improves numerical accuracy with the trade-off of less detailed anatomical representation. A positive side effect is that the computational time is reduced when the smoothing algorithm is applied. The performance of the smoothing algorithm was confirmed by comparison with analytic solutions in a head-like layered sphere. The algorithm was tested for both uniform and localized magnetic-field exposures of anatomically realistic head models.

When the smoothing algorithm was applied for anatomical head models, the 99th percentile values stayed relatively constant independent of the amount of smoothing. Consequently, the maximum electric field values after smoothing provide a conservative estimate for the non-smoothed 99th percentile value. This is especially useful for localized exposure cases where the 99th percentile can underestimate real exposure by a factor of three (in the studied cases) and possibly more in different exposure scenarios such as in the one studied in Kos *et al* (2011). For uniform exposure at the ICNIRP (2010) reference levels, not only the 99th percentile but also the smoothed maximum induced electric fields were in compliance with the basic restriction limits.

Details of the anatomical model are lost when the smoothing algorithm is applied, so the smoothing volume should be as small as is enough for removing the worst staircasing errors. It should be noted that the smoothed conductivity might still fall within the range of uncertainty of low-frequency conductivity values (Gabriel *et al* 2009). Smoothing the conductivity values over a voxelized sphere of radius of 3 to 4 cells seemed to provide very good numerical accuracy for a grid resolution of 2 mm, as shown by comparison with the analytic solution in a layered sphere (section 3.1). More anatomical accuracy could be obtained by using a higher resolution anatomical model, because the physical smoothing volume would be smaller for the same number of voxels.

Acknowledgements

The authors wish to thank the Finnish Cultural Foundation and the Academy of Finland for financial support.

References

Bahr A, Bolz T and Hennes C 2007 Numerical dosimetry Elf: Accuracy of the method, variability of models and parameters, and the implication for quantifying guidelines *Health Phys.* **92**(6) 521–30

Caputa K, Dimbylow P J, Dawson T W and Stuchly M A 2002 Modelling fields induced in humans by 50/60 Hz magnetic fields: reliability of the results and effects of model variations *Phys. Med. Biol.* **47**(8) 1391–8

Dawson T and Stuchly M 1998 High-resolution organ dosimetry for human exposure to low-frequency magnetic fields *IEEE Trans. Magnetics* **34**(3) 708–18

Dawson T W, Caputa K and Stuchly M A 1997 Influence of human model resolution on computed currents induced in organs by 60-Hz magnetic fields *Bioelectromagnetics* **18**(7) 478–90

Dawson T W, Moerloose J D and Stuchly M A 1996 Comparison of magnetically induced ELF fields in humans computed by FDTD and scalar potential FD codes *Appl. Comput. Elecromagn. Soc. J.* **11**(3) 63–71

Dawson T W, Potter M and Stuchly M A 2001 Evaluation of modeling accuracy of power frequency field interactions with the human body *Appl. Comput. Elecromagn. Soc. J.* **16**(2) 162–72

Dimbylow P 2005 Development of the female voxel phantom, NAOMI, and its application to calculations of induced current densities and electric fields from applied low frequency magnetic and electric fields *Phys. Med. Biol.* **50**(6) 1047–70

Dimbylow P and Findlay R 2010 The effects of body posture, anatomy, age and pregnancy on the calculation of induced current densities at 50 Hz *Radiation Protection Dosimetry* **139**(4) 532–8

Dimbylow P J 1998 Induced current densities from low-frequency magnetic fields in a 2 mm resolution, anatomically realistic model of the body *Phys. Med. Biol.* **43**(2) 221–30

Gabriel C, Peyman A and Grant E H 2009 Electrical conductivity of tissue at frequencies below 1 MHz *Phys. Med. Biol.* **54**(16) 4863–78

Gabriel S, Lau R W and Gabriel C 1996 The dielectric properties of biological tissues: III. Parametric models for the dielectric spectrum of tissues *Phys. Med. Biol.* **41**(11) 2271–93

Hirata A, Takano Y, Fujiwara O, Dovan T and Kavet R 2011 An electric field induced in the retina and brain at threshold magnetic flux density causing magnetophosphenes *Phys. Med. Biol.* **56**(13) 4091–101

Hirata A, Takano Y, Kamimura Y and Fujiwara O 2010 Effect of the averaging volume and algorithm on the in situ electric field for uniform electric- and magnetic-field exposures *Phys. Med. Biol.* **55**(9) N243–52

Hirata A, Wake K, Watanabe S and Taki M 2009 In-situ electric field and current density in japanese male and female models for uniform magnetic field exposures *Radiation Protection Dosimetry* **135**(4) 272–75

ICNIRP 2010 Guidelines for limiting exposure to time-varying electric and magnetic fields (1 Hz to 100 kHz) *Health Phys.* **99**(6) 818–36

IEEE 2002 IEEE Standard for Safety Levels with Respect to Human Exposure to Electromagnetic Fields, 0-3 kHz, C95.6-2002 (New York: Institute of Electrical and Electronics Engineers)

Ilvonen S and Laakso I 2009 Computational estimation of magnetically induced electric fields in a rotating head *Phys. Med. Biol.* **54**(2) 341–51

Kos B, Valič B, Miklavčič D, Kotnik T and Gajšek P 2011 Pre- and post-natal exposure of children to EMF generated by domestic induction cookers *Phys. Med. Biol.* **56**(19) 6149–60

Nagaoka T, Watanabe S, Sakurai K, Kunieda E, Watanabe S, Taki M and Yamanaka Y 2004 Development of realistic high-resolution whole-body voxel models of Japanese adult males and females of average height and weight, and application of models to radio-frequency electromagnetic-field dosimetry *Phys. Med. Biol.* **49**(1) 1–15

Nishizawa S, Landstorfer F and Kamimura Y 2007 Low-frequency dosimetry of inhomogeneous magnetic fields using the coil source model and the household appliance *IEEE Trans. Biomed. Eng.* **54**(3) 497–502

Yamazaki K, Kawamoto T, Fujinami H and Shigemitsu T 2004 Equivalent dipole moment method to characterize magnetic fields generated by electric appliances: extension to intermediate frequencies of up to 100 kHz *IEEE Trans. Electromagn. Compat.* **46**(1) 115–20